PAPER Special Section on Mobile Information Network

The Spread Spectrum Code Hopping System

Takeshi ONIZAWA†, *Associate Member and* Takaaki HASEGAWA†, *Member*

SUMMARY In this paper, the spread spectrum code hopping (CH) system, which has some analogy to frequency hopping systems, is described. The CH system has robustness to code interference that restriction of kinds of PN matched filters (MFs) will cause. The mean acquisition time is shown by theoretical analysis and computer simulation. The acquisition rate results under a single code interference, which seriously affects direct sequence systems, and an asynchronous two-user channels are obtained. Moreover, using theoretical analysis and computer simulation, the bit error rate (BER) performance under single code interference is evaluated. It is shown that CH systems perform better than conventional ones under single code interference.

key words: *spread spectrum, code hopping, code interference, mobile, consumer*

1. Introduction

Communication systems have been changing; in particular, recently mobile communication systems toward integrated information networks have rapidly developed. Interference, multipath and fading are serious problems for the mobile communication systems. Therefore, Spread Spectrum (SS)[1]techniques have attracted attention for mobile communication applications[2].

On the other hand, since demands of communications have become diversified, consumer communications become popular systems. In addition, high reliability under poor channels at low cost is required on consumer communications. SS communication systems have also been applied to consumer communications[3].

SS communication systems are mainly divided into two categories based on modulation, i.e., direct sequence (DS) and frequency hopping (FH). For simple implementation, DS systems are widely used, however the DS signals can be easily demodulated by delay detection techniques.

As mentioned above, SS communication systems have started to be widely used in mobile and consumer communications. In these systems, PN codes are assigned to each user and are administrated within each communication area. In future, completely administrated communication systems such as cellular phone systems and non-officially administrated communication systems such as consumer communications[3] are expected to confuse. Therefore, independently administrated wireless information networks are expected to be near mutually. From the point of view of hardware, we can get just limited kinds of surface-acoustic-wave (SAW) MFs for PN codes. The situation will cause us to use the same code coincidentally at an overlapped or neighboring area shown in Fig. 1.

Even if the same code is used, more than one chip difference enables DS systems to communicate. However, considering code acquisition[4]–[6] (data symbol synchronization), it is not always true. The reason is as follows: for example, let us assume that only area B's users communicate using PN_i, after that, area A's users start to communicate using the same code as shown in Fig. 1. Before starting communication, code acquisition is required; if area B's transmitter is very near, the user represented as the black circle cannot capture area A's PN_i transmitted from far place in area A. In this case, area A's receiver captures area B's PN_i instead of area A's PN_i. Therefore, such code interference is serious for DS systems, and is expected to happen in future. Code interference in DS systems corresponds to narrow-band interference in narrow-band systems.

On the other hand, FH systems are robust to narrow-band interference because of use of various carrier frequencies. The use of various frequencies makes communication systems robust, the use of various PN codes may similarly make DS systems powerful.

In this paper, we apply the idea of changing carrier frequencies to that of changing spreading codes to suppress code interference. We call it the spread spectrum code hopping (CH) system[8],[9]; it has the analogy to the FH system on hopping. A similar system for security, which differs greatly from our purpose, was proposed previously[7]. The paper discusses from the viewpoint of sequences.

This paper is organized as follows: Sect. 2 describes

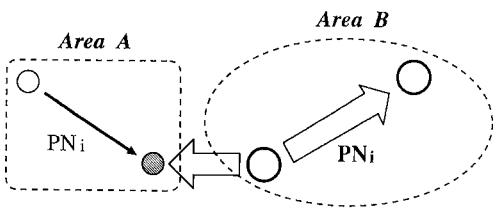

Fig. 1 Code interference from a neighboring area.

Manuscript received November 16, 1994.
Manuscript revised February 14, 1995.

†The authors are with the Faculty of Engineering, Saitama University, Urawa-shi, 338 Japan.

the CH system. Section 3 discusses code acquisition. Single user channel performance is given in Sect. 4. Conclusions are then presented in the last section.

2. The Code Hopping System

2.1 Code Hopping

This subsection describes the principle of the CH system. Table 1 shows notations used in the following discussions. Figure 2 illustrates various types of SS systems; (a), (b) and (c) represent DS, FH and CH systems, respectively. The shade of (b) represents narrow-band interference and that of (c) does code interference. The symbol (+ or −) in each small square in Fig. 2 represents transmitted data. In Fig. 2 (a) and (c) both the systems use Sequence Inversion Keying (SIK) every three periods of PN codes. Figure 2 (b) indicates the case of one data modulation per three frequency hopping periods. In the FH system, if one hopping frequency is affected by single narrow-band interference, another hopping frequency is not affected by that. Hence, the FH system has robustness to narrow-band interference.

In the CH system, let us assume the worst case that an interference code is one of the prepared spreading codes; both on the timing (PN code's phase) and clock rate, the interference code synchronizes with one of the prepared spreading codes. Therefore, since an interference code affects mainly the same spreading code's MF, the CH system provides robustness to code interference similar to the FH system.

From general meaning, the CH system may be considered as the system in which data modulates short part (after this, we call it a unit code.) of a long PN code. However, the CH system is different from such a system on the following points :

1. Every PN code (unit code) used in the CH system is widely used one, that is, such a long code consists of well-used short PN codes.
2. Mod/Demod is based on each unit code, which is very short compared with the long code.
3. If the hopping pattern is not periodical, the spreading code, which consists of well-used short unit codes whose device is easy to get, has an infinite period.

The explicit hopping of well-used short codes is the insisted point. Furthermore, in the CH system, the spreading code is determined by both of the unit codes and a hopping pattern. Therefore, all of the users use almost the same hardware that consists of all kinds of the unit codes and one particular hopping pattern.

Table 1 Notations.

K	Number of Prepared Spreading Codes
N	Number of Hops per data symbol
M	Decision Ratio of Majority Rule

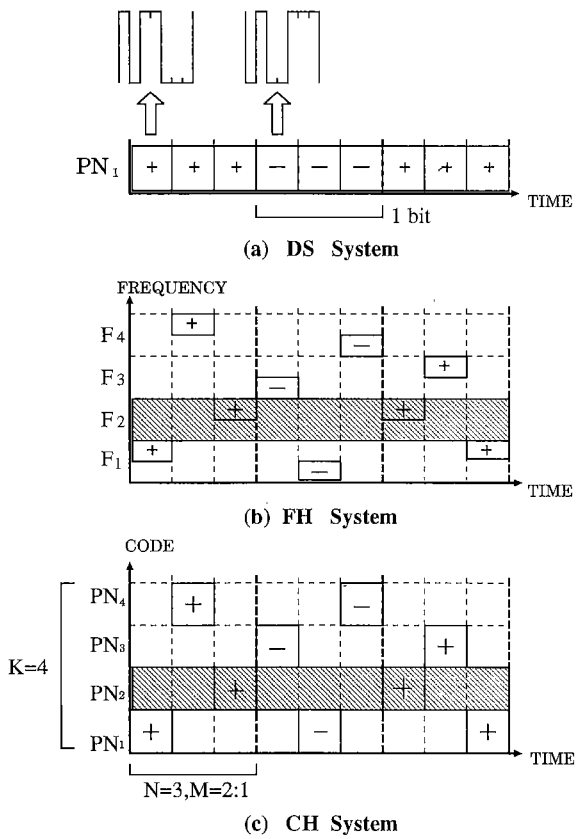

Fig. 2 SS systems.

2.2 System Structure

A block diagram of the CH system is shown in Fig. 3. Different hopping patterns are assigned to all the users one another for multiple access like FH systems.

In the transmitter, the spreading code is switched according to a hopping pattern. Additive white gaussian noise (AWGN) and an interference code add to the CH signals. In the receiver, active or passive correlation is carried out to demodulate data.

3. Code Acquisition Performance

This section considers a code acquisition problem of the CH system. We theoretically derived mean acquisition time under an AWGN channel using the schemes described in Refs. [5], [6]. Furthermore, We estimate acquisition rate performance under two conditions, one is a single code interference channel and the other is an asynchronous two-user channel both by theory and simulation. Table 2 shows the simulation conditions.

3.1 Acquisition System Description

A block diagram of the code acquisition scheme for the CH system is shown in Fig. 4. MFs are used to detect each unit code. Output signals of the MFs are delayed

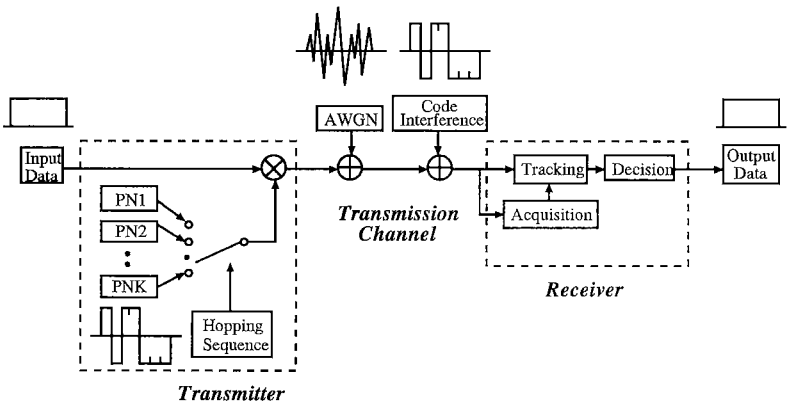

Fig. 3 A block diagram of the CH system.

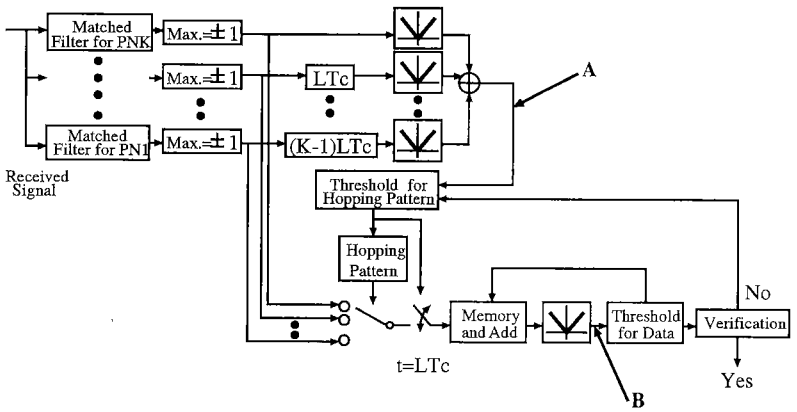

Fig. 4 A block diagram of the code acquisition scheme for the CH system.

and added corresponding to a hopping pattern. Hence, the device will produce a large output signal when a corresponding hopping pattern is input. Limiters are used to prevent a single strong interference code from causing a large false output. We let the amplitude of the desired signal be $+1$ or -1 for simplicity.

Moreover, data symbol synchronization is required after hopping pattern synchronization. For data symbol synchronization, a data pattern that appears $+1, -1$ by turns is employed. In the CH system, the process of data symbol synchronization is not always started after that of the hopping pattern synchronization immediately. Therefore, this acquisition system tries to find data symbol using shifting of sampling timing. The search procedure of the acquisition system for data symbol shown in Fig. 5 is explained as follows: The system carries out N times tests for searching data symbol. If the data symbol is not found, the system returns to the mode of hopping pattern synchronization. Conversely, if the system can detect a data symbol, it stops shifting sampling timing and moves to the verification mode. Therefore, Fig. 5 shows the case that after two times of shifting the system can capture data symbol, where $K = 4$ and $N = 3$. The confirmation condition of acquisition in the verification mode is based on a majority rule. We call the number of test counts A; A tests are

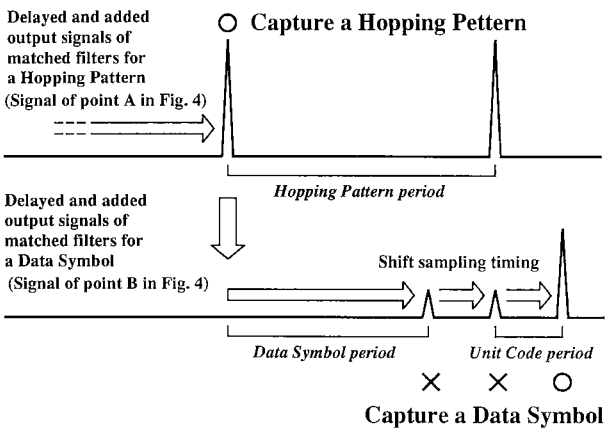

Fig. 5 An example of search procedure of the CH system with $K = 4$ and $N = 3$.

repeated in the verification mode. If at least B of A tests indicate data symbol synchronization, we assume that the acquisition process is over.

3.2 Mean Acquisition Time

We apply Polydoros and Weber's theory [5], [6] to this receiver. Due to the Markovian nature of the acqui-

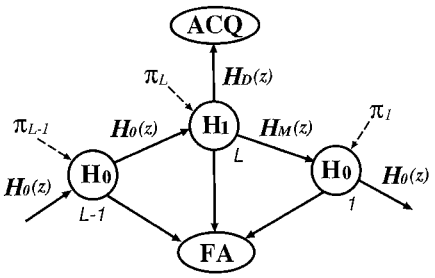

Fig. 6 A flow graph diagram of hopping pattern synchronization.

sition process, the flow graph diagram can be used in deriving mean acquisition time. As mentioned above, the system synchronizes a hopping pattern first. A flow graph diagram of hopping pattern synchronization is shown in Fig. 6. Each state corresponds to the timing of a unit code for simplicity. In the following, H_1 denotes the states that a hopping pattern is synchronized and H_0 represents the alternative states. The two remaining states are correct-acquisition (ACQ) and false-alarm (FA) states respectively, as shown in Fig. 6. Therefore the total number of states is $L+2$ where L is unit code length. Moreover we assume that the initial relative position of the codes is set as worst-case location, according to the initial distribution $(\pi_1 = 1, \pi_j = 0; j \neq 1)$.

Here let us assume z to the unit-delay operator. If the unit delay specifically corresponds to τ seconds, where τ is time of one chip length T_c, z is replaced by z^τ in the following discussion. Furthermore, we assign more general gains $H(z)$ to the different branches in Fig. 6 as follows: $H_D(z)$ is the gain of the branch leading from H_1 to the ACQ; $H_M(z)$ represents the gain of the branch connecting H_1 with H_0 while $H_0(z)$ is the gain of the branch connecting any other two successive states $(i, i+1); i = 1, \cdots, L-1$.

Moreover, we need to consider data symbol synchronization. In the Appendix, data symbol synchronization is discussed. The gains $H_D(z)$, $H_M(z)$ and $H_0(z)$ are derived in the Appendix to be given (A· 6), (A· 7) and (A· 8), respectively.

Furthermore, after using loop reduction method, the generating function is defined by

$$P_{ACQ}(z) = \frac{H_D(z)H_0^{L-1}(z)}{1 - H_M(z)H_0^{L-1}(z)}. \tag{1}$$

Moreover, the overall detection probability is denoted by

$$P_D^{ov} = P_{ACQ}(z)\,|_{z=1}\,. \tag{2}$$

Therefore, mean acquisition time $E\{T_{acq}\}$ is derived by

$$E\{T_{acq}\} = \frac{dP_{ACQ}(z)}{dz}\,|_{z=1}\,. \tag{3}$$

Here, let us assume $X1$ to be a total output signal of MFs. We can comment relation between a probability for a first dwell P_{X1} and a probability for the verification dwell P_{X2}, P_{X2} is given by

$$P_{X2} = \sum_{n=B}^{A} \binom{A}{n} P_{X1}^n (1 - P_{X1})^{A-n}. \tag{4}$$

A probability P_{X1} is defined by

$$P_{X1} = \int_{Th}^{\infty} p_{X1}(x)dx \tag{5}$$

with a threshold of each situation Th and a probability density function $p_{X1}(x)$. $p_{X1}(x)$ is computed directly in this acquisition system.

In the following, we consider mean acquisition time performance under an AWGN channel. Figure 7 shows the mean number of data symbol $E\{T_{acq}\}/LNT_c$, versus the normalized threshold of a hopping pattern Th_{hop}. We set $A = 4$, $B = 2$, A is the number of test counts on the verification mode, and the normalized threshold of data symbol $Th_{data} = 0.7$. It is clear from Fig. 7 that an optimal threshold with minimizes $E\{T_{acq}\}/LNT_c$ exists for each value of E_b/N_0, where E_b/N_0 is the ratio of energy per data symbol to

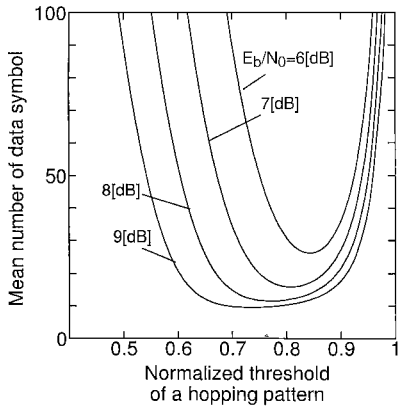

Fig. 7 Mean number of data symbol $E\{T_{acq}\}/LNT_c$ vs. the normalized threshold of a hopping pattern Th_{hop} with $A = 4, B = 2$ and $Th_{data} = 0.7$.

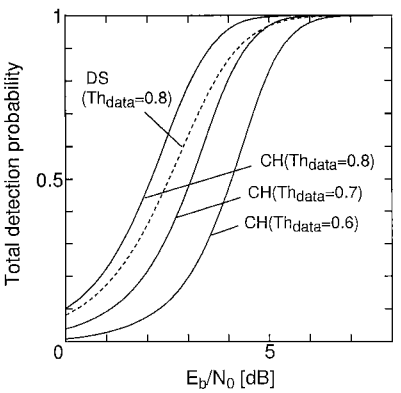

Fig. 8 Total detection probability P_D^{ov} vs. E_b/N_0 with $A = 4, B = 2$ and $Th_{hop} = 0.8$.

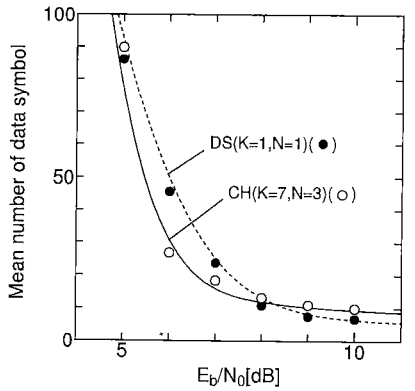

Fig. 9 Mean number of data symbol $E\{T_{acq}\}/LNT_c$ vs. E_b/N_0 with $A = 4$ and $B = 2$.

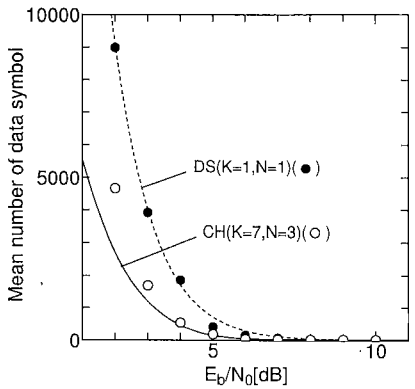

Fig. 10 Mean number of data symbol $E\{T_{acq}\}/LNT_c$ vs. E_b/N_0 with $A = 20$ and $B = 10$.

single-sided thermal white noise spectral density. However, for simplicity we use fixed value for the normalized threshold of a hopping pattern Th_{hop} is 0.8.

Figure 8 indicates the total detection probability P_D^{ov} versus E_b/N_0 with $A = 4$, $B = 2$ and $Th_{hop} = 0.8$. We select that Th_{data} for DS systems is 0.8 from the theoretical analysis. Since the condition of the CH system is roughly equal to that of DS systems, we let Th_{data} for the CH system to be 0.7. In the following discussion, $Th_{hop} = 0.8$, $Th_{data} = 0.7$ are used for the CH system, and $Th_{data} = 0.8$ is used for DS systems.

Figure 9 depicts the mean number of data symbol versus E_b/N_0 with $A = 4$ and $B = 2$. The performance of the CH system is the same as that of DS systems. In Figs. 9 and 10, curves are theoretical analysis and dots represent simulated values.

Next, considering the synchronization for low E_b/N_0, we shows the mean number of the data symbol versus E_b/N_0 with $A = 20$ and $B = 10$ in Fig. 10. The acquisition performance of the CH system is superior to that of DS systems in this case. DS systems searches timing of data symbol serially. On the other hand, the CH system has hopping pattern synchronization, and

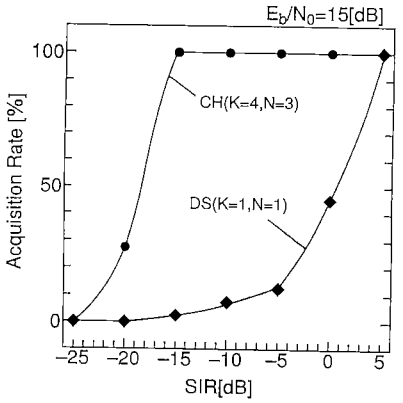

Fig. 11 Acquisition rate vs. SIR under single code interference with $E_b/N_0 = 15$ [dB].

searches timing of data symbol under the high detection probability of data symbol. As we set the value of A is high, this effect of the CH system becomes remarkable. However, since we ignore the cross-correlation magnitude of output signals on MFs in derivation of the probability density function $p_{X1}(x)$, the difference between the theoretical value and the simulated ones of the CH system is caused by the ignorance.

3.3 Acquisition Rate

We estimate the acquisition rate performance under a single code interference channel and an asynchronous two-user channel. From the previous section, the parameter under the two conditions is as follows: $Th_{hop} = 0.8$, $Th_{data} = 0.7$ for the CH system, $Th_{data} = 0.8$ for DS systems, and $A = 20$, $B = 10$ for both systems.

Figure 11 shows the acquisition rate versus SIR under single code interference with $E_b/N_0 = 15$ [dB]. E_b/N_0 is the ratio of energy per data symbol to single-sided thermal white noise spectral density. SIR is the desired user to a interference user energy ratio per data symbol duration of the desired user. DS systems tend to capture an interference code with increasing energy of the interference code. However, the CH system keeps good performance under single code interference. We note that about 18 [dB] performance improvement of the CH system is obtained under the acquisition rate = 50 [%].

Figure 12 illustrates the acquisition rate versus SIR under an asynchronous two-user channel with $E_b/N_0 = \infty$ [dB]. In Fig. 12, SIR is the ratio of the energy per data symbol of the desired user to that of the second user. In this case, the Reed-Solomon code whose code length=7 is assigned to each user for the hopping pattern. From Fig. 12, it is clear that the CH system is robuster than DS systems. We can see that the performance improvement is about 3 [dB] under the acquisition rate = 50[%]. Because the improvement is caused by the hopping pattern synchronization of the CH sys-

tem. Here, we consider DUR, which is the power ratio of the desired signal to the signal of second user, at the decision timing of a hopping pattern. We assume one data per three unit codes in this case. The interference power of MF output is proportional to the interference power of MF input. As expected, the desired signal power of MF output is in proportion to the desired signal amplitude of MF input. Let DUR_{unit}, DUR_{DS} and DUR_{CH} denote the power ratio of the desired signal to the signal of the second user. The DUR of DS systems are expressed as

$$DUR_{DS} = 3 \cdot DUR_{unit}, \tag{6}$$

where DUR_{unit} is the energy ratio of the desired signal to the signal of the second user per unit code. Similarly, the DUR of the CH system is given by

$$DUR_{CH} = 7 \cdot DUR_{unit}, \tag{7}$$

where the number of prepared spreading codes $K = 7$. (6) and (7) can be combined into

$$DUR_{CH} = \frac{7}{3} DUR_{DS}. \tag{8}$$

We calculate that $10\log_{10} 7/3 \cong 3.7\,[\mathrm{dB}]$. Therefore, it is considered that the robustness of the CH system in a two-user channel is the improvement of DUR at the decision timing of a hopping pattern.

4. BER Performance under Single User Channels

In this section, we discuss the situation after the acquisition process mentioned above. A single interference code is coincident with one of the prepared spreading codes, i.e., the worst case. We carried out theoretical analysis and simulation of the CH systems both for majority rule decision scheme, which is widely used in fast FH systems, and the sum decision scheme.

4.1 Performance Analysis

4.1.1 Majority Rule Decision

Considering a desired channel and a code interference, the cross-correlation magnitude of code interference have 2 states on each data symbol. Using the cross-correlation magnitude of code interference for the kth unit code in the jth state $\hat{C}_{kj}$, and the number of hops per data symbol N, we obtain the error rate of the kth unit code, $P_k^{(j)}$, as

$$P_k^{(j)} = Q\left\{\sqrt{\frac{2E_b}{NN_0}}\left(1 + \sqrt{\frac{E_{int}}{E_b}}\hat{C}_{kj}\right)\right\}$$

$$k = 1, 2, \cdots, N \tag{9}$$

where E_{int} denotes energy per data duration of the interference code; it is assumed that in our discussion data duration of the interference code is equal to data symbol duration of the desired signal. E_b is the energy per data symbol. E_b/E_{int} is equivalent to SIR. N_0 is the single-sided thermal white noise spectral density.

When the majority of N unit codes errors, the data symbol error occurs. Let $P_{ex}^{(j)}$ represent the bit error rate of the $(1, 2, \cdots, \frac{LCM[K,N]}{N}) = x$th data symbol where $LCM[K, N]$ is the period of the hopping pattern, under the cross-correlation magnitude of code interference in the jth state. For example, when $N = 3$, bit error rate of the first data symbol, $P_{e1}^{(j)}$, is calculated to be

$$\begin{aligned} P_{e1}^{(j)} &= P_1^{(j)}P_2^{(j)}P_3^{(j)} + P_1^{(j)}P_2^{(j)}\left(1 - P_3^{(j)}\right) \\ &+ P_1^{(j)}\left(1 - P_2^{(j)}\right)P_3^{(j)} + \left(1 - P_1^{(j)}\right)P_2^{(j)}P_3^{(j)}. \end{aligned} \tag{10}$$

Hence, the average bit error rate of the xth data symbol, P_{ex}, can be expressed as

$$P_{ex} = \frac{1}{2}\sum_{j=1}^{2} P_{ex}^{(j)}, \quad x = 1, 2, \cdots, \frac{LCM[K,N]}{N}. \tag{11}$$

Let us consider the period of the hopping pattern, the average bit error rate for the hopping pattern, P_e, is given by

$$P_e = \frac{N}{LCM[K,N]} \sum_{x=1}^{\frac{LCM[K,N]}{N}} P_{ex}. \tag{12}$$

4.1.2 Sum Decision

Similarly, the correlation magnitudes of code interference have 2 states on each data symbol. Using the cross-correlation magnitude of code interference for each data symbol in the jth state $\hat{C}_j$, and the number of hops per data symbol N, average bit error rate of the xth data symbol, P_{ex}, is denoted by

$$P_{ex} = \frac{1}{2}\sum_{j=1}^{2} Q\left\{\frac{1}{N}\sqrt{\frac{2E_b}{N_0}}\left(N + \sqrt{\frac{E_{int}}{E_b}}\hat{C}_j\right)\right\}$$

$$x = 1, 2, \cdots, \frac{LCM[K,N]}{N}. \tag{13}$$

Here the period of the hopping pattern is considered. By substitution of (13), we obtain the average bit error rate for the hopping pattern, P_e, as shown in (12).

4.2 Performance Comparison

We carried out simulations to evaluate the performance of the CH system under single code interference to verify

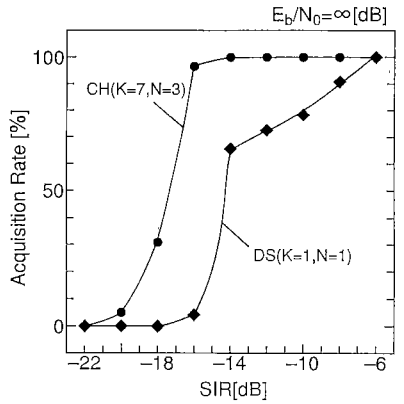

Fig. 12 Acquisition rate vs. SIR under an asynchronous two-user channel with $E_b/N_0 = \infty$ [dB].

Table 2 Simulation conditions.

Spreading Code	Maximal-Length Sequence
Code Length	127
Interference Code	One of Prepared Spreading Codes • The Same Clock Rate (Acquisition performance simulation) • The Same Clock Rate and Timing (BER performance simulation)
Noise	Additive White Gaussian Noise
Detection	Coherent Detection (BER performance simulation)
Synchronization	Ideal (BER performance simulation)

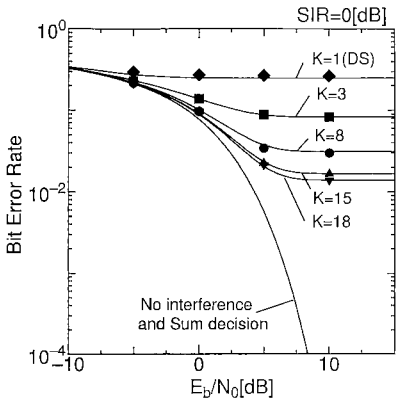

Fig. 13 Bit error rate vs. E_b/N_0 with $N = 1$ and $SIR = 0$ [dB].

the theoretical analysis noted on the previous section. The simulation conditions are shown in Table 2. The curves in the following figures represent theoretical values; simulated values are expressed as plots.

Figure 13 illustrates the BER versus E_b/N_0 with the number of hops per data symbol $N = 1$ and $SIR = 0$ [dB]. In this figure, the BER of the usual DS system ($K = 1$) is about 0.25. However, since the effect of single code interference decreases with increasing the number of prepared spreading codes K, the performance is improved.

Figure 14 shows the BER versus E_b/N_0 with $K = 3$, $N = 3$ and $SIR = 0$ [dB]. The DS system is affected by code interference similarly. On the other hand, the floors of the BER in Fig. 14 vanish and the performance is improved drastically. We note that increase of N is effective for performance improvement. The performance of the sum decision scheme is better than that of the majority rule one where $K = 3$, $N = 3$ and $SIR = 0$ [dB].

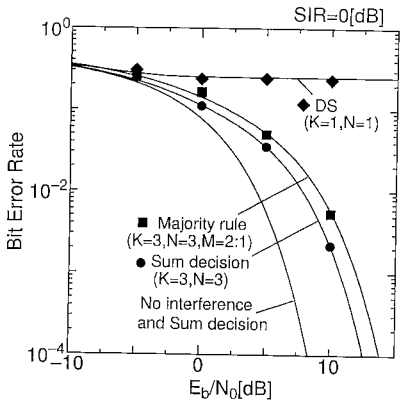

Fig. 14 Bit error rate vs. E_b/N_0 with $K = 3$, $N = 3$ and $SIR = 0$ [dB].

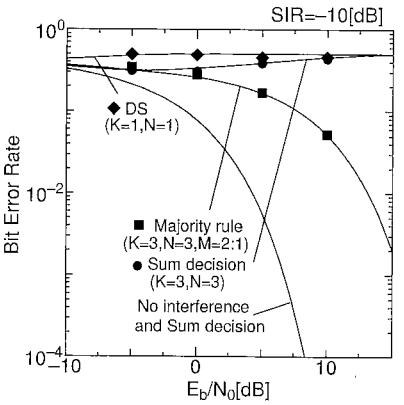

Fig. 15 Bit eror rate vs. E_b/N_0 with $K = 3$, $N = 3$ and $SIR = -10$ [dB].

Figure 15 shows the same situation as Fig. 14 except $SIR = -10$ [dB]. The energy of the code interference is larger than that of the previous case. Therefore, code interference has a strong effect on the DS system. In the CH system, the sum decision scheme is based on linear summation of each component per data symbol duration. Therefore, if the interference is extremely strong, the performance of the sum decision scheme is strongly affected by single code interference similar to the DS system. However, since the hard limiter of each unit code restricts the effect of code interference to only one unit decision, the performance of the majority rule decision scheme is better than that of the sum decision scheme under such code interference.

Finally, Fig. 16 depicts the BER versus E_b/N_0 with $K = 15$, $N = 13$ and $SIR = -10$ [dB]. The performances of the sum and majority rule schemes shown

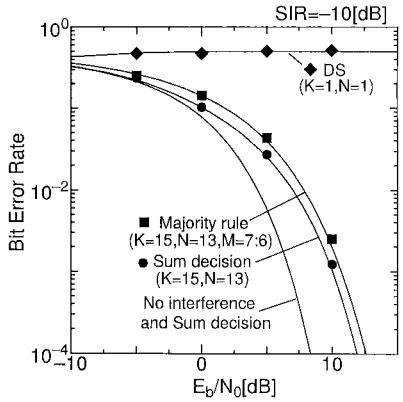

Fig. 16 Bit eror rate vs. E_b/N_0 with $K = 15$, $N = 13$ and $SIR = -10$ [dB].

in Fig. 16 are better than those of both schemes shown in Fig. 15. Though the energy of code interference is large, increase of K and N is effective for performance improvement. Here, let us explain the reason of selecting $K = 15$, $N = 13$ in Fig. 16. We must consider hits in code division multiple access (CDMA) of the CH system similar to FH/CDMA systems. Therefore, to decrease probabilities of hits in CH/CDMA systems, we used a Reed-Solomon code whose code length = 15 as a hopping pattern; $K = 15$. Moreover, since the majority rule decision scheme requires that N is an odd number, we set $N = 13$ as an instance.

These simulated values are in good agreement with the theoretical ones through these figures. The principal conclusion here is that, as expected, if we use a number of PN codes, the increasing the number of prepared spreading codes K and number of hops per data symbol N improves the performance of the CH system, where the energy of code interference changes drastically. When we can select just limited kinds of PN codes, the majority rule decision is better scheme.

5. Conclusions

In this paper, we discussed the spread spectrum code hopping system. The CH system hops spreading codes as FH systems hop the carrier frequencies. First, code acquisition performance was studied. The CH system indicated better performance in mean acquisition time. In Fig. 11, the acquisition rate performance of the CH system under single code interference that will happen in future is shown. About 18 [dB] performance improvement is characterized. Moreover, the CH system had robustness in an asynchronous two-user channel. Second, BER performance evaluation was carried out in a single user channel. It was shown that the CH system can communicate under single code interference that seriously affects DS systems. It has been concluded that the CH system is superior to DS systems under single code interference. Performances in CDMA and fading channels are our future works.

Acknowledgment

We gratefully acknowledge useful discussion of Prof. M. Nakagawa of Keio University, Dr. Y. Nakagawa of Ricoh Co.,Ltd., and the staff of Hasegawa Lab. We also would like to thank Prof. M. Haneishi of Saitama University for his encouragement throughout this work.

References

[1] Pickholtz, R.L., Schilling, D.L. and Milstein, L.B., "Theory of Spread-Spectrum Communications – A Tutorial," *IEEE Trans. Commun.*, vol.COM-30, pp.855–884, May 1982.
[2] Cooper, G.R. and Nettleton, R.W., "A Spread-Spectrum Technique for High-Capacity Mobile Communications," *IEEE Trans. on Vehicular Technology*, vol.VT-27, pp.264–275, Nov. 1978.
[3] Nakagawa, M. and Hasegawa, T., "Spread Spectrum for Consumer Communications – Applications of Spread Spectrum Communications in Japan –," *IEICE Trans.*, vol.E74, pp.1093–1102, May 1991.
[4] Rappaport, S.S. and Grieco, D.M., "Spread-Spectrum Signal Acquisition: Methods and Technology," *IEEE Commun. Mag.*, vol.22, pp.6–21, Jun. 1984.
[5] Polydoros, A. and Weber, C.L., "A Unified Approach to Serial Search Spread-Spectrum Code Acquisition – Part I: General Theory," *IEEE Trans. Commun.*, vol.COM-32, pp.542–549, May 1984.
[6] Polydoros, A. and Weber, C.L., "A Unified Approach to Serial Search Spread-Spectrum Code Acquisition – Part II: A Matched-Filter Receiver," *IEEE Trans. Commun.*, vol.COM-32, pp.550–560, May 1984.
[7] Suehiro, N., Koshida, I. and Hatori, M., "Code Hopping SSMA System Using Modulatable Orthogonal Sequence for Information Traffic Security," *IEICE Technical Report*, SS87-10, 1987.
[8] Hasegawa, T. and Onizawa, T., "The Spread Spectrum Code Hopping System," *IEICE Technical Report*, SST92-72, 1993.
[9] Onizawa, T. and Hasegawa, T., "The Spread Spectrum Code Hopping System," in *Proc. IEEE ISSSTA '94*, pp.287–291, Jul. 1994.

Appendix: Derivation of the Gains of $H_D(z)$, $H_M(z)$ and $H_O(z)$

In this appendix, we consider data symbol synchronization and derive the gains $H_D(z)$, $H_M(z)$ and $H_O(z)$ shown in Fig. 6.

First of all, the upper part of Fig. A· 1 shows a flow graph diagram of data symbol synchronization corresponding to Fig. 5, and black circles are the states that acquisition system traces in Fig. 5. Let us name this situation *case*3. *case*3 is explained as the case that the system can detect data symbol on the third sampling timing after two times of shifting. In other words, Fig. A· 1 shows a detail of one part on $H_D(z)$ and $H_M(z)$ in Fig. 6.

P_H is the detection probability of a hopping pattern. Furthermore, (P_{d1}, P_{s1}) and (P_{d2}, P_{s2}) denote the detection probability of the data symbol and the false

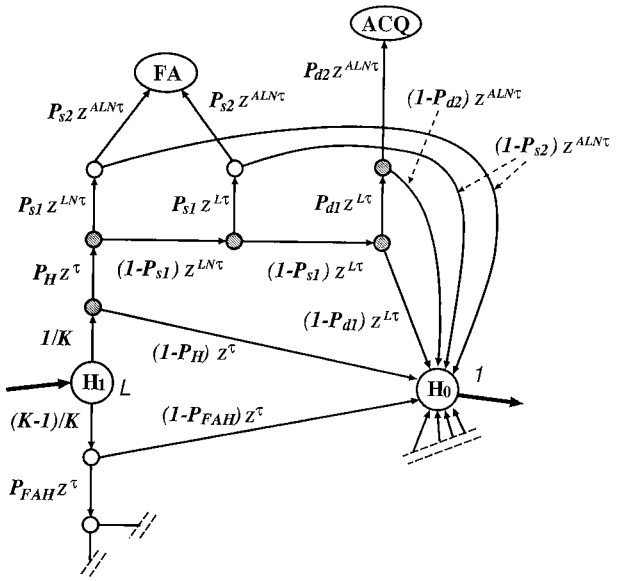

Fig. A· 1 A flow graph diagram of the data symbol synchronization for *case* 3 with $N = 3$.

detection probability of the data symbol pairs for the first and verification dwells, respectively. We will explain the difference between P_{d1} and P_{s1} in previous Fig. 5. P_{d1} denotes the detection probability of the large peak, and P_{s1} is the false detection probability of the small peak.

Using these probabilities, we can write the gains for *case* 3 as

$$H_{D3main}(z) = \frac{1}{K}P_H(1-P_{s1})^2P_{d1}P_{d2} \cdot z^{\{1+2L+(1+A)LN\}\tau} \quad (A\cdot 1)$$

and

$$\begin{aligned} H_{M3main}(z) = {} & \frac{1}{K}(1-P_H)\cdot z^{\tau} \\ & + \frac{1}{K}P_H P_{s1}(1-P_{s2}) \cdot z^{\{1+(1+A)LN\}\tau} \\ & + \frac{1}{K}P_H(1-P_{s1})P_{s1}(1-P_{s2}) \cdot z^{\{1+L+(1+A)LN\}\tau} \\ & + \frac{1}{K}P_H(1-P_{s1})^2P_{d1}(1-P_{d2}) \cdot z^{\{1+2L+(1+A)LN\}\tau} \\ & + \frac{1}{K}P_H(1-P_{s1})^2(1-P_{d1}) \cdot z^{(1+2L+LN)\tau}. \end{aligned} \quad (A\cdot 2)$$

case 1 is the case that ,after hopping pattern synchronization, the system can detect data symbol at the first sampling timing. Moreover, *case* 2 is the case that the system captures data symbol at the second sampling timing after one time of shifting.

Similarly, we can derive H_{D1main} and H_{M1main} for *case* 1 , as

$$H_{D1main}(z) = \frac{1}{K}P_H P_{d1}P_{d2} \cdot z^{\{1+(1+A)LN\}\tau}. \quad (A\cdot 3)$$

and

$$\begin{aligned} H_{M1main}(z) = {} & \frac{1}{K}(1-P_H)\cdot z^{\tau} \\ & + \frac{1}{K}P_H P_{d1}(1-P_{d2}) \cdot z^{\{1+(1+A)LN\}\tau} \\ & + \frac{1}{K}P_H(1-P_{d1})P_{s1}(1-P_{s2}) \cdot z^{\{1+L+(1+A)LN\}\tau} \\ & + \frac{1}{K}P_H(1-P_{d1})(1-P_{s1})P_{s1} \cdot (1-P_{s2})\cdot z^{\{1+2L+(1+A)LN\}\tau} \\ & + \frac{1}{K}P_H(1-P_{d1})(1-P_{s1})^2 \cdot z^{(1+2L+LN)\tau}. \end{aligned} \quad (A\cdot 4)$$

However, at the state L in Fig. 6, the mode of data symbol synchronization happens to start before hopping pattern synchronization is not complete because of the false alarm probability of a hopping pattern P_{FAH}. Therefore, we consider data symbol synchronization of N cases caused by the false alarm probability of a hopping pattern similarly. The lower part of Fig. A· 1 shows a flow graph diagram of data symbol synchronization for *case* 3 with $N = 3$ due to P_{FAH},

The gain for the *case*3 caused by P_{FAH}, $H_{D3sub}(z)$, is given by

$$H_{D3sub}(z) = \frac{(K-1)}{K}P_{FAH}(1-P_{s1})^2P_{d1}P_{d2} \cdot z^{\{1+2L+(1+A)LN\}\tau}. \quad (A\cdot 5)$$

$H_{D1sub}(z), H_{D2sub}(z)$ is obtained similarly.

In general, using the before method, we get $H_{D1main}(z)$, $\cdots$, $H_{DNmain}(z)$ and $H_{D1sub}(z)$, $\cdots$, $H_{DNsub}(z)$.

Therefore, $H_D(z)$ and $H_M(z)$ are defined by

$$\begin{aligned} H_D(z) = {} & \frac{1}{N}(H_{D1main}(z) + H_{D2main}(z)+,\cdots, \\ & +H_{DNmain}(z)) \\ & + \frac{1}{N}(H_{D1sub}(z) + H_{D2sub}(z)+,\cdots, \\ & +H_{DNsub}(z)). \end{aligned} \quad (A\cdot 6)$$

and

$$\begin{aligned} H_M(z) = {} & \frac{1}{N}(H_{M1main}(z) + H_{M2main}(z)+,\cdots, \\ & +H_{MNmain}(z)) \\ & + \frac{1}{N}(H_{M1sub}(z) + H_{M2sub}(z)+,\cdots, \\ & +H_{MNsub}(z)). \end{aligned} \quad (A\cdot 7)$$

Next, we derive the gain of the branch connecting any other two successive states H_0. P_{FA1} and P_{FA2} are the false alarm probability of data symbol for the first and verification dwells, respectively. For example, using P_{FA1}, P_{FA2} and the false alarm probability of a hoppin g pattern P_{FAH}, H_0 with $N = 3$ is expressed as

$$\begin{aligned} H_0(z) = {} & (1 - P_{FAH}) \cdot z^{\tau} \\ & + P_{FAH} P_{FA1} (1 - P_{FA2}) \cdot z^{\{1+(1+A)LN\}\tau} \\ & + P_{FAH} (1 - P_{FA1}) P_{FA1} (1 - P_{FA2}) \\ & \quad \cdot z^{\{1+L+(1+A)LN\}\tau} \\ & + P_{FAH} (1 - P_{FA1})^2 P_{FA1} (1 - P_{FA2}) \\ & \quad \cdot z^{\{1+2L+(1+A)LN\}\tau} \\ & + P_{FAH} (1 - P_{FA1})^3 \cdot z^{(1+2L+LN)\tau}. \quad \text{(A·8)} \end{aligned}$$

Finally, we can derive that the gains $H_D(z)$, $H_M(z)$ and $H_0(z)$ are (A·6), (A·7) and (A·8), respectively.

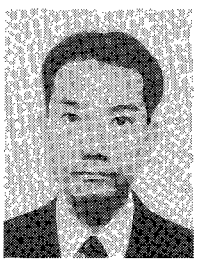

Takeshi Onizawa was born in Yokohama, Japan, on May 16, 1969. He received the B.E. and M.E. degrees in Electrical Engineering from Saitama University in 1993 and 1995. His research interest is in Spread Spectrum Communications.

Takaaki Hasegawa was born in Kamakura, Japan, on July 4, 1957. He received the B.E., M.E. and Ph.D. degrees in Electrical Engineering from Keio University, in 1981, 1983 and 1986, respectively. He joined in Faculty of Engineering, Saitama University in 1986. Since 1991 he has been an associate professor. His research interests are in Spread Spectrum Communications, Signal Processing and Human Communications. Dr. Hasegawa is a member of IEEE and SITA of Japan.